

Chapter 11

Grid Integration of Large-Scale Electric Vehicles: Enabling Support Through Power Storage

Prateek Jain and Trapti Jain

11.1 Comparing the Greenhouse Gas (GHG) Emissions of Electric Vehicles (EV) and Conventional Internal Combustion Engine (ICE) Vehicles: A Large-Scale Perspective

Various energy losses occur at every single stage of fuel life cycle, i.e., in delivering fuel from primary (ultimate) source to final conversion into vehicular motion. For example, energy is expended, and emissions take place in the extraction of crude oil, combustion of fossil fuels, etc. in the whole operation of internal combustion engine (ICE) vehicles, whereas losses occur in generating electricity from various sources, its transmission and distribution, utilization in charging the battery, etc. during the whole operation of an electric vehicle (EV). The life cycle energy and greenhouse gas (GHG) assessment, popularly known as well-to-wheel analysis, is carried out to assess the environmental impact of the above two vehicular technologies. It consists of two stages: (1) well-to-tank—an upstream stage, and (2) tank-to-wheel—the downstream stage. The well-to-tank stage involves evaluating the energy dissipated and the associated GHG emissions in delivering the refined fuel from the primary source into onboard (tank) the vehicle. The tank-to-wheel refers to evaluating the exhausted energy and associated GHG emissions from the fuel onboard the vehicle in achieving a particular driving range. The addition of the estimates of the two stages will give the total well-to-wheel energy expenditure and associated GHG emissions.

P. Jain (✉) · T. Jain

Discipline of Electrical Engineering, Indian Institute of Technology Indore,
Simrol, Indore, 453552, MP, India

Table 11.1 Vehicle data

Electric vehicle (EV) Tesla (2017)	
Electric car model	Tesla Model S
Battery capacity (kWh)	75
Average speed (miles per hour)	45
Distance possible with the battery capacity at average speed (miles)	393
ICE vehicle parameters equivalent of EV	
Average fuel economy (miles per gallon (MPG))	25
Gallons of gasoline required for 393 miles	15.72

In this section, a comparison of fuel life cycle GHG emissions from the battery electric vehicles (BEV) and that of equivalent ICE vehicles during the whole operation has been made. A Tesla Model S with a typical battery capacity of 75 kWh has been selected as a representative BEV. Based on the selected BEV, the equivalent ICE vehicle parameters were devised. A total of 0.2 million representatives BEVs and hence the equivalent ICE vehicles are assumed considering a mid-size city for the comparison. The assumed scenario on vehicle data has been listed in Table 11.1.

The well-to-wheel energy usage and GHG emissions for the above two categories of vehicles are discussed below.

11.1.1 Battery Electric Vehicle (BEV)

Table 11.2 summarizes well-to-wheel energy expenditure and GHG emission analysis for the considered scenario of EVs. The two comprising stages in the assessment are as follows:

11.1.1.1 Well-to-Tank Assessment

While charging a battery, some of the power is utilized in pushing the electrons through the battery, decreasing the actual energy being stored and available for driving. The typical number for this loss in the battery is 10% Markowitz (2013). The average electricity transmission and distribution (T&D) losses as estimated by the US Energy Information Administration (EIA) EIA (2017a) is about 5% of the electricity that is transmitted and distributed annually in the USA. Based on this information, the T&D losses while supplying the charging energy to the battery of an EV are taken as 5%. Adding the above two gives a total 15% losses. Thus, for a given EV capacity of 75 kWh, the energy corresponding to 86.25 kWh has to be supplied from the sources mix to meet these losses. The major sources of electricity generation in the USA at utility-scale facilities in 2016 EIA (2017b) as well as the life cycle GHG emissions by each source (in g CO₂/kWh) Edenhofer et al (2012) are

Table 11.2 Well-to-wheel analysis of electric vehicles (EV)

Stage 1: Well-to-tank				
Sources/ technology	Percentage generation	Gram CO ₂ /kWh	kWh from each sources	Gram CO ₂ emission
Coal	30.4	1001	26.22	26,246.22
Natural gas	33.8	469	29.1525	13,672.5225
Nuclear	19.7	16	16.99125	271.86
Hydroelectric	6.5	4	5.60625	22.425
Wind	5.6	12	4.83	57.96
Solar	0.9	46	0.77625	35.7075
Biomass	1.5	18	1.29375	23.2875
Geothermal	0.4	45	0.345	15.525
Stage 2: Tank-to-wheel				
Electric vehicles emit no gasses at all at the point of operation, i.e., CO ₂ emissions = 0				
Total GHG emissions under the assumed scenario				
GHG emissions per vehicle (g)				4.0345 × 10 ⁴
GHG emissions of 0.2 million EVs (kg)				8.0691 × 10 ⁶

summarized in Table 11.2. It can be correlated that the above energy of 86.25 kWh per EV is supplied via these sources as per their percentage shares in the generation mix. From this, the gram CO₂ emission per vehicle from these sources for the total energy supplied can be evaluated as recorded in Table 11.2. The total well-to-tank GHG emissions per vehicle are found to be 40.345 kg.

11.1.1.2 Tank-to-Wheel Assessment

The BEVs are zero emission vehicles as no gases are generated at the point of operation. The batteries are sealed, having a gel with no harmful fumes produced Sachin (2015). Therefore, the tank-to-wheel GHG emissions from the BEVs can be treated as zero. Hence, the overall GHG emissions of 0.2 million BEVs as considered in the scenario is estimated as 8.0691×10^6 kg.

11.1.2 Internal Combustion Engine (ICE) Vehicle

Table 11.3 summarizes well-to-wheel energy dissipation analysis for the ICE vehicles scenario equivalent of considered EVs. Again, the two comprising stages in the assessment are as follows:

Table 11.3 Well-to-wheel analysis of ICE equivalent of EV

Stage 1: Well-to-tank					
GHG emissions from crude oil production			GHG emissions from petroleum refining		
Source	Emission (g/gallon crude)	Emission per vehicle (g/gallon crude)	Source	Emission (g/gallon crude)	Emission per vehicle (g/gallon crude)
ROG	0.7	11.004	ROG	0.2	3.144
CO	0.3	4.716	CO	0.5	7.86
NO _x	0.3	4.716	NO _x	0.4	6.288
			SO _x	0.7	11.004
Stage 2: Tank-to-wheel					
CO ₂ emissions per gallon of gasoline (g)					8887
CO ₂ emission per vehicle (g)					139,703.64
Total GHG emissions under the assumed scenario					
Well-to-tank GHG emissions per vehicle (g)					48.732
Tank-to-wheel GHG emissions per vehicle (g)					1.3970×10^5
GHG emissions of 0.2 million ICE vehicles (kg)					2.79504×10^7

11.1.2.1 Well-to-Tank Assessment

An equivalent ICE vehicle having the same driving range (393 miles) as of the considered EV above would require 15.72 gallons of gasoline with an average fuel economy of 25 miles per gallon (MPG) Naughton (2015). Now, there are GHG emissions accompanied with crude oil production and then from petroleum refining to feed these gallons of gasoline onboard tank of the vehicle. The various emissions per ICE vehicle along with their sources considering crude oil production TIAX LLC (2007) and petroleum refining TIAX LLC (2007) in this stage are quantified in Table 11.3.

11.1.2.2 Tank-to-Wheel Assessment

The grams of CO₂ dissipated per gallon of gasoline combustion is evaluated by multiplying the heat content of the gasoline per gallon with the kg CO₂ per heat content of the fuel. The conversion factor of 8887 g of CO₂ Federal Register (2010) emissions per gallon of gasoline consumed have been taken as the standard assuming all the carbon in the gasoline is converted to CO₂ Eggleston et al (2006). Using this factor, the CO₂ emissions per ICE vehicle which is consuming 15.72 gallons of gasoline can be evaluated as shown in Table 11.3. The sum of well-to-tank and tank-to-wheel GHG emissions would yield total life cycle GHG emissions, which is found to be 2.79504×10^7 kg with 0.2 million ICE vehicles equivalent of the considered scenario of EVs.

From the above assessment of life-cycle GHG emissions for the two categories of vehicular technology, it can be concluded that an internal combustion engine vehicle emits about 3.5 times the emissions with the equivalent driving range

battery electric vehicle. As per International Energy Agency (IEA) IEA (2011), transportation sector alone accounts for 30% of global energy consumption, being the second largest source of CO₂ emissions contributing to 20% of global GHG emissions. Also, it is anticipated that there will be a tremendous increase in energy consumption in the transportation with growing demand for personal vehicles EIA (2013). Hence, transportation electrification with growing use of EVs presents excellent prospects for reducing the discharge of CO₂ and other toxic GHG, apart from saving the depleted stock of fossil fuels. Further, these benefits will increase manifold if renewable energy sources are being exploited to the fullest to charge the batteries of this energy efficient breed of vehicles.

11.2 Development of Charging Load Profiles of Electric Vehicles¹

In order to ascertain whether the existing grid capacity will be able to support additional EV load with random charging, the assessment of charging load profiles based on the driving pattern of the owners is integral. The selection of charging power magnitude among the existent charging standards as well as the charging physics plays a crucial role in shaping the load profiles generated by the EVs. In this regard, this part analyzes the charging load profiles of the large-scale EVs employing the possible combinations of charging physics of constant time (CT) charging and constant power (CP) charging Darabi and Ferdowsi (2011) along with two distinct charging rates of 3.3 and 6.6 kW.

11.2.1 Process of Developing the Charging Load Profiles

11.2.1.1 Electric Vehicle Characteristics

Three types of EVs are considered. Their relevant characteristics and composition percentages RWTH (2010) in the system are detailed in Table 11.4. The Battery Electric Vehicle (BEV) and City-BEV are fully electric vehicles powered solely by the onboard battery. The PHEV 90, carrying an electric range of 90 km is a hybrid electric vehicle having ICE as a range extender unit. A total of 0.17 million vehicles is assumed in the system for the case study. Based on the vehicles' characteristics and composition percentages in the system, the weighted average values for the assumed scenario are also summarized in Table 11.4.

¹Section adapted from work published by the authors in reference Jain and Jain (2014a).

Table 11.4 Characteristics of electric vehicles

Type of vehicle	Battery capacity (kWh)	Consumption (kWh/km)	All-electric range (km)	Composition (%)
BEV	35	0.20	175	37
City-BEV	16	0.12	133	10
PHEV 90	18	0.20	90	53
Weighted average values				
Battery capacity (kWh)				24
Consumption (kWh/km)				0.192
All-electric range (km)				125

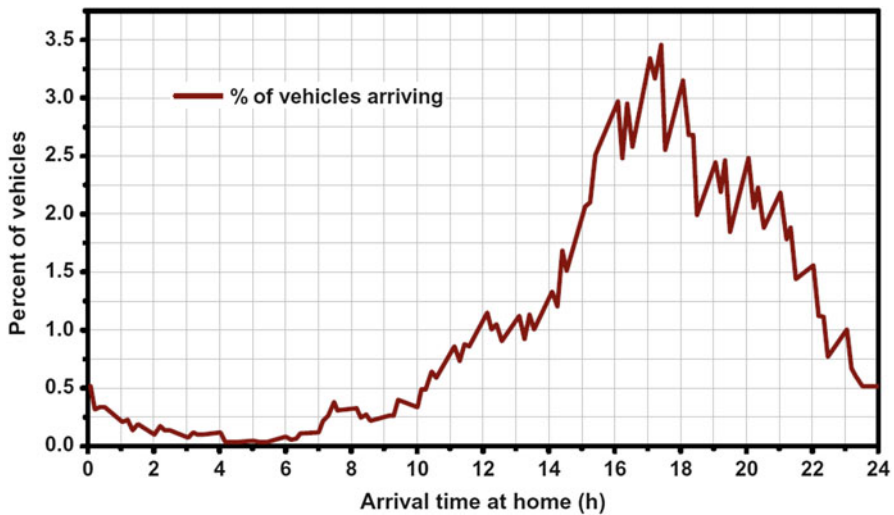


Fig. 11.1 Final arrival times of vehicles at home

11.2.1.2 Arrival Pattern

Figure 11.1 shows the percentage of vehicles arriving against their final arrival times at home. The arrival pattern has been developed taking the data inputs from Darabi and Ferdowsi (2011); NHTS (2001). The final arrival time of the vehicles has been treated as the charging start time because it is inferential that the commuters would plug their vehicles for charging soon after arriving at home. It can be observed that higher percentages of vehicles are arriving at home in the evening and late evening hours characterizing the routine driving behavior of commuters, returning to home from work or other related trips.

Table 11.5 Electric vehicle charging standards

SAE J1772 standard			
Charging type	Voltage level	Power level	Phase
Level 1	120 V AC	1.2–2.0 kW	Single-phase
Level 2 (low)	208–240 V AC	2.8–3.8 kW	Single-phase
Level 2 (high)	208–240 V AC	6.0–19.2 kW	Single-phase
Level 3	208–240 V AC	15–96 kW	3-phase
DC charging (level 1, 2 and 3)	200–600 V DC	>15–240 kW	DC
EPRI charging standard			
Charging type	Electrical ratings		
AC level 1	120 V AC, 12–16 A, 1.44–1.92 kW, single-phase		
AC level 2	208–240 V AC, 12–80 A, 2.5–19.2 kW, single-phase		
DC level 1, 2 and 3	200–600 V DC, ≤ 80 –400 A, ≤ 19.2 – ≤ 240 kW		

11.2.1.3 Charging Standards

The two EV charging standards namely SAE J1772 Kalhammer et al (2009) and EPRI-NEC Duvall and et al (2011) are summarized in Table 11.5. However, both the standards are proportionate seeing the electrical ratings of voltage, current, and power. Most of the contemporary charging infrastructure are suited for domestic AC low charging, as well as the worldwide top selling model of electric cars, supports charging with SAE J1772 AC Level 1 or 2 connectors up to 6.6 kW. Installation of DC fast charging (DCFC) station for typical residential applications is debatable because, first, its setup is very expensive, and second, there will be a huge burden of utility-scale distribution capacity upgradation in order to allow such a huge amount of power to flow through the distribution end power equipment. Considering this, the charging power levels of 3.3 and 6.6 kW, considering AC level 2 (low) and level 2 (high) of both the standards, are taken to develop the load profile of the EVs. With every hour of charging, these power levels add an electric range of approximately 17 and 34 km, respectively.

11.2.1.4 Charging Physics

Constant Time (CT) Charging Approach In constant time charging approach Darabi and Ferdowsi (2011), the total charging time is a fixed duration and is decided by the charging power standard for a given battery. This results in variation of charging power as per the SOC of the battery. For example, a battery with capacity 24 kWh has fixed charging time of 7.3 and 3.6 h, respectively with a given charging power standards of 6.6 and 3.3 kW.

Constant Power (CP) Charging Approach In this approach Darabi and Ferdowsi (2011), the charging power is fixed at the level specified. So, the charging time varies depending upon the SOC of the battery. Thus, the charging power levels of 3.3 and 6.6 kW results in a maximum charging time of 7.3 and 3.6 h, respectively, for an average battery capacity of 24 kWh.

11.2.1.5 Energy Required from the Grid

The arrival times of the vehicles are discretized into four arrival times per hour, and hence a total 96 arrival times throughout the day. Within the average all-electric range of 125 km (Table 11.4), the vehicles were classified into various driven distance groups (n). Finally, the driven distance groups are dispersed into the considered arrival times of the vehicles throughout the day. Electrical energy is consumed by the vehicles in driving, causing depleted energy state of the battery. This energy state is specified by the term state of charge (SOC). The SOC of a battery is expressed as the percentage of the energy state of a fully charged battery. For example, a vehicle driven completely to its capacity (up to AER) would carry 0% SOC. Likewise, a vehicle driven half of its AER would carry a SOC of 50%. The charging energy required to bring the battery back to the full is the complement of this SOC.

The charging energy required by the EVs from the grid at various arrival times of the day will be:

$$E^t = \sum_{m=1}^n (d_m^t \times n_m^t \times E_{\text{avg}}) \quad \forall t \in (1, 2, \dots, 96) \quad (11.1)$$

where E^t is the charging demand of EV aggregation arriving at time t , d_m^t is the driven distance by the m^{th} distance group of vehicles arriving at time t , n_m^t is the number of m^{th} distance group of vehicles arriving at time t , and E_{avg} is the average energy consumed by the vehicle.

11.2.2 The Charging Load Profiles

The charging load profiles of EVs as realized with the possible combination of charging power levels and charging physics are shown in Fig. 11.2. It has been considered that the vehicles start charging as soon as they arrive at home after finishing the trip(s). Figure 11.2 contains all the charging curves, i.e., the profiles obtained by employing the two charging powers of 6.6 and 3.3 kW individually with the constant time (CT) and constant power (CP) approaches. It can be observed that the load curves with CT approach are less peaking as compared to the load curves with CP approach for both the power levels. Similarly, for both the charging approaches, the load curves of 3.3 kW power level has lesser peak value when compared with the load curves of 6.6 kW charging power level. In addition to this, the peaks with CT scheme are shifted toward the right in comparison to the peaks with CP scheme for both the charging powers. Likewise, for both the charging schemes, the peaks with a lesser charging power of 3.3 kW is shifted toward the right in contrast to the charging load peaks caused by the 6.6 kW power level. The above two features are summarized quantitatively in Table 11.6. This is so,

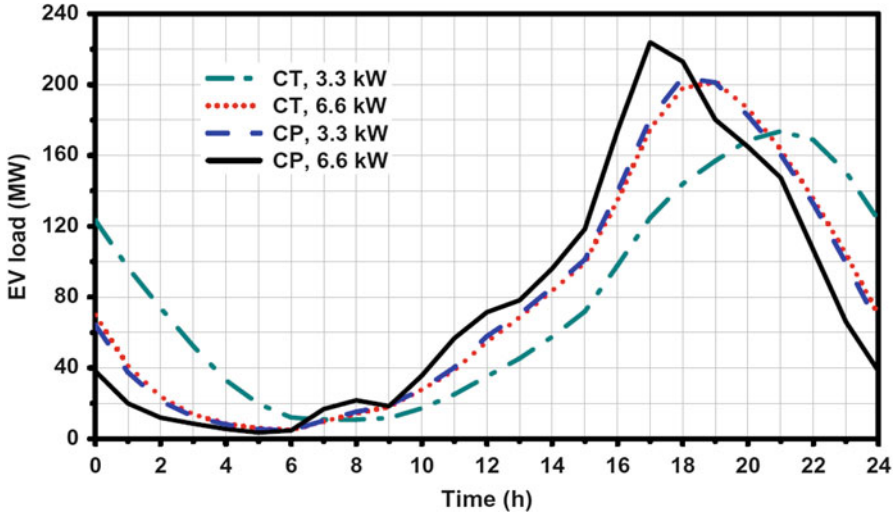


Fig. 11.2 Charging load profiles of EVs under various approaches

Table 11.6 Features of charging load curves of EVs

Charging level (kW)	Charging approach			
	Constant power (CP)		Constant time (CT)	
	Peak load (MW)	Peak time	Peak load (MW)	Peak time
3.3	204	18:00	174	21:00
6.6	224	17:00	202	19:00

as, for a given amount of charging energy required from the grid as per the SOC of the vehicles arriving, use of high charge power level would supply the energy fast (in a lesser time), resulting in an increased peak that too near the arrival time of the vehicles. Also, in constant power charging approach, the charging power is constant whereas the charging time is being scaled as per the SOC of the vehicle, causing fast charging of vehicles in opposition to constant time charging approach, where the charging power is being scaled down to lower values in order to keep the total charging time a fixed duration. Thus, it can be concluded that the load is more peaking as well as drifted toward early hours with a combination of high charge power level with constant power charging approach, increasing the degree of fluctuation. In opposition to this, the load profiles originating from a combination of low charge power level with constant time charging approach are the flatter ones, as the peak is less as well as shifted toward late hours.

11.3 V2G and G2V Profiles Under Varying Equilibrium of EV Aggregation²

In transportation, the average car is parked almost 90% of the time leaving enormous time margin during the day to exploit the storage potential of the battery for grid support services. This led the researchers to propose the vehicle-to-grid (V2G) mode of operation of EVs in which a proportion of energy stored in the battery (after accounting for driving consumption) can be injected back into the grid as an aggregated storage device. In view of this, in this section V2G profiles are developed with various discharge power levels characterizing the mobility behavior. The heterogeneity in the vehicles as well as in the mobility behavior is also incorporated to determine the grid-to-vehicle (G2V) and V2G power capabilities of the aggregation at different moments of parking under varying penetrations of the electric vehicles. The quantification of the effects of the simultaneous combination of resulting G2V and V2G profiles with the conventional load on hourly loading and electricity market price is presented taking IEEE Test Bus system as an example.

11.3.1 Mobility Attributes

Four specimens EVs, namely BEV, City-BEV, PHEV 90, and PHEV 30, for representing the small, medium, and large version of electric cars in the market are considered as shown in Table 11.7. Speed dependent energy consumption of EVs considering four different phases of driving Pasaoglu et al (2012); RWTH (2010) viz. road, downtown, highway, and traffic for each of the four vehicles have been modeled. Three penetration percentages 25, 50, and 100% for the presence of EVs in the customer segment are created, and the proportion of various electric cars at these penetration levels was varied. Again, the total number of EVs are assumed to be 0.17 million (at 100% penetration). The percentage proportions in EV adoption at various penetration levels are influenced by several factors like socioeconomic capability, charging infrastructure availability, the cost of EVs, etc. Based on the above factors, RWTH (2010) presented a trend of adoption figures of EVs in various proportions which formed the basis for the selection of above composition percentages of various EVs at these penetration levels. In this case, 120 distance groups of vehicles, from 1 to 196 km, are considered. Also, it is supposed that, distance groups of EVs up to 67 km complete 40% of their trip on the road, 30% from downtown, 20% on the expressway, and remaining 10% in moving through traffic. The remaining distance groups, from 67 to 196 km, are assumed to perform 40% of their travel on the expressway, 30% from downtown, 20% on the road, and the remaining 10%

²Section adapted from work published by the authors in references Jain and Jain (2016) and Jain and Jain (2014b).

Table 11.7 Mobility attributes

Vehicle type	Battery capacity (kWh)	Energy consumption (kWh/km)			All-electric range (km) (based on 80% DoD)			Percentage composition			Driving course	Speed range (kmph)		
		Road	Downtown	Expressway	Traffic	Road	Downtown	Expressway	Traffic	25%			50%	100%
BEV	35	0.130	0.181	0.209	0.212	215	154	134	132	32	45	37	Road	55–67
City-BEV	16	0.120	0.167	0.193	0.195	107	76	66	65	20	12	10	Downtown	35–43
PHEV 90	18	0.150	0.209	0.241	0.244	96	69	60	59	24	21.5	26.5	Expressway	80–98
PHEV 30	12	0.150	0.209	0.241	0.244	64	46	40	39	24	21.5	26.5	Traffic	21–27

in traffic driving. This is to signify that the trips with short distances are mainly taking place in the urban zone while the trips with large distances include a high proportion of transit through expressways. The depth-of-discharge of the battery in driving as well as V2G supply is limited up to 80% in the analysis with a purpose of EV owners' obligation of maintaining a reasonable battery lifetime, as deep charge-discharge cycles shorten the battery life. Based on the premise, the weighted average parameters of the aggregation at the three penetration scenarios of 25, 50, and 100% are summarized in Table 11.8.

11.3.2 Development of V2G and G2V Profiles

11.3.2.1 Energy Consumption in Driving

The energy consumed in driving by the EV aggregation of 120 distance groups arriving at various (96) arrival times through the day is given by:

$$E^\tau = \sum_{m=1}^{120} (\alpha + \beta + \gamma + \delta) \quad \forall \tau \in (1, 2, \dots, 96) \quad (11.2)$$

where,

$$\alpha = 0.4 | 0.2 \begin{cases} pc_m^\tau (k_m^{\tau R} \cdot E_{avg}^R) & \forall k_m^{\tau R} \leq AER_{avg}^R \\ \left\{ \begin{array}{l} pc_m^\tau (AER_{avg}^R \cdot E_{avg}^R) \\ \{0\} \end{array} \right. & \forall k_m^{\tau R} > AER_{avg}^R \\ \{0\} & \forall \text{ BEVs and City - BEVs} \end{cases} \quad (11.2.1)$$

$$\beta = 0.3 \begin{cases} pc_m^\tau (k_m^{\tau D} \cdot E_{avg}^D) & \forall k_m^{\tau D} \leq AER_{avg}^D \\ \left\{ \begin{array}{l} pc_m^\tau (AER_{avg}^D \cdot E_{avg}^D) \\ \{0\} \end{array} \right. & \forall k_m^{\tau D} > AER_{avg}^D \\ \{0\} & \forall \text{ BEVs and City - BEVs} \end{cases} \quad (11.2.2)$$

$$\gamma = 0.2 | 0.4 \begin{cases} pc_m^\tau (k_m^{\tau E} \cdot E_{avg}^E) & \forall k_m^{\tau E} \leq AER_{avg}^E \\ \left\{ \begin{array}{l} pc_m^\tau (AER_{avg}^E \cdot E_{avg}^E) \\ \{0\} \end{array} \right. & \forall k_m^{\tau E} > AER_{avg}^E \\ \{0\} & \forall \text{ BEVs and City - BEVs} \end{cases} \quad (11.2.3)$$

Table 11.8 Scenario description

Penetration ratio	Average battery capacity (kWh)		Average energy consumption (kWh/km)				Average all-electric range (km)			
	80% DoD	100% DoD	Road	Downtown	Expressway	Traffic	Road	Downtown	Expressway	Traffic
25%	17.697	22.113	0.1376	0.1916	0.2212	0.2240	129	92	80	79
50%	19.771	24.728	0.1374	0.1914	0.2208	0.2237	144	103	90	88
100%	18.543	23.196	0.1396	0.1944	0.2244	0.2273	133	95	83	81

$$\delta = 0.1 \begin{cases} pc_m^\tau (k_m^{\tau\text{Tr}} \cdot E_{\text{avg}}^{\text{Tr}}) & \forall k_m^{\tau\text{Tr}} \leq \text{AER}_{\text{avg}}^{\text{Tr}} \\ pc_m^\tau (\text{AER}_{\text{avg}}^{\text{Tr}} \cdot E_{\text{avg}}^{\text{Tr}}) & \forall k_m^{\tau\text{Tr}} > \text{AER}_{\text{avg}}^{\text{Tr}} \\ \{0\} & \forall \text{BEVs and City} - \text{BEVs} \end{cases} \quad (11.2.4)$$

Here, E^τ is the energy consumed in driving by the EVs arriving at time τ and pc_m^τ is the percentage of m^{th} mileage group of vehicles arriving at time τ . Further, $k_m^{\tau R}$, $k_m^{\tau D}$, $k_m^{\tau E}$, and $k_m^{\tau\text{Tr}}$ are the km traveled by m^{th} mileage group of vehicles arriving at time τ , respectively, while moving through road, downtown, expressway, and traffic driving periods; $\text{AER}_{\text{avg}}^R$, $\text{AER}_{\text{avg}}^D$, $\text{AER}_{\text{avg}}^E$, and $\text{AER}_{\text{avg}}^{\text{Tr}}$ are the average values of all-electric range (AER) given by vehicles; and E_{avg}^R , E_{avg}^D , E_{avg}^E , and $E_{\text{avg}}^{\text{Tr}}$ are the average values of energy consumed in driving per km by the vehicles, respectively, when they move through road, downtown, expressway, and traffic driving periods. The figures 0.4, 0.3, 0.2, and 0.1 signify the travel percentage of vehicles, respectively for the driving periods road, downtown, expressway, and traffic for mileage groups with short trips (up to 67 km). Though, these figures are 0.2, 0.3, 0.4, and 0.1, correspondingly for these driving courses for mileage groups with long trips (above 67 km). The computation yields energy required by the EVs in driving along the number of vehicles arriving at various arrival times. Given the total storage capacity of the aggregation, the complement of the energy required for the driving is the net available energy for V2G supply.

11.3.2.2 V2G and G2V Moments

The mobility pattern of vehicles is defined by considering only work purpose trips in which vehicles commute between home and workplace. Thus, the G2V and V2G moments can be ascertained, once the arrival and departure times, travel and parking duration, as well as the commute circuit are fixed. This analysis accounts the average workplace parking duration to be 7 h Pasaoglu et al (2012) and average commuting duration 1.3 h, resulting in 15.7 h of average home parking time. It is hypothesized that the vehicles are plugged into the grid at workplace only soon after their arrivals to supply V2G power, while they are connected to the grid for charging (G2V) as soon as they finally arrive at home to bring the battery back to the full. Figure 11.1 shows the pattern of the final arrival time of vehicles at home. By employing the workplace parking and commuting duration Pasaoglu et al (2012) as considered above, the pattern of arrival of vehicles at the workplace can be obtained, which is shown in Fig. 11.3. A greater concentration of final arrivals of vehicles at home exists in the evening hours, though the concentration shifts into morning hours for the arrivals at the workplace, characterizing the regular office/work timings. Each distance group of vehicles was split into the considered 96 arrival times in the same proportions as derived from the arrival patterns.

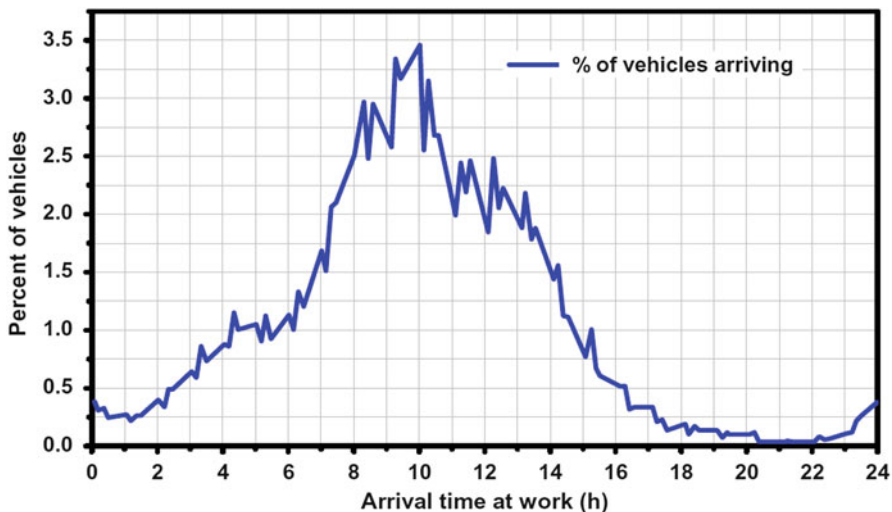


Fig. 11.3 Arrival times of vehicles at work

Table 11.9 Charging time duration and electric range added

Charging power (kW)	Charging time duration (h)						Electric range added per hour of charging (km)		
	Constant power (CP)			Constant time (CT)			25%	50%	100%
	25%	50%	100%	25%	50%	100%			
2.5	4.8	5.5	5.0	8.8	9.9	9.3	13.9	14.0	13.7
3.3	3.6	4.2	3.8	6.7	7.5	7.0	17.4	18.4	18.1
6.6	1.8	2.1	1.9	3.3	3.7	3.5	36.8	36.9	36.3

11.3.2.3 Charging and Discharging Power Levels

The V2G profiles have been realized with the discharge power levels of 1.44, 1.64, 1.92, 2.5, 3.3, and 6.6 kW, which covers both AC Level 1 and AC Level 2 range of SAE J1772 Kalhammer et al (2009) and EPRI Duvall and et al (2011) charging standards. However, the G2V profiles have been developed with charging power levels of 2.5, 3.3, and 6.6 kW only, which also comprise AC Level 1 and 2 of the two charging standards. The charging power cannot be selected below 2.5 kW in this study because of the constraint of 15.7 h available maximum charging time at home to bring the battery back to the full. The electric range added per hour of charging with these charging powers is shown in Table 11.9.

11.3.2.4 Charging and Discharging Approach

The nonlinear charging characteristics of a typical Li-ion battery consist of two stages of charging. The first stage is the constant current (CC) stage Simpson

(2011); Young et al (2013) which is analogous to constant power (CP) charging Darabi and Ferdowsi (2011) and persists till the battery is about 70% charged. In this stage, charging current remains constant, while the battery voltage rises to the reference voltage limit. This results in variable charging time depending upon the SOC of the battery as discussed in Sect. 11.2.1.4. The second stage takes over after it and lasts till the battery is fully charged. This stage is called constant voltage (CV) stage Simpson (2011); Young et al (2013) and is analogous to constant time (CT) charging Darabi and Ferdowsi (2011) approach. During this stage, the charging current decays exponentially (power scaling) resulting in a high charging time in comparison to the CC stage. Considering this, the G2V (charging) profiles of the aggregation have been developed considering charging from 0 to 70% battery capacity through constant power (CP) approach, while the next 70 to 100% capacity through constant time (CT) approach. The charging times with the two approaches at various charge power levels are listed in Table 11.9.

11.3.3 V2G and G2V Profiles of the Aggregation

11.3.3.1 V2G Profiles

Figure 11.4 shows the V2G profiles of the aggregation at the two terminal discharge power levels of 1.44 and 6.6 kW of the considered range under the three penetration scenarios. A range buffer corresponding to 20 km Pasaoglu et al (2012) as well as vehicle-grid interfacing converter efficiency of 93% has been assumed while evaluating the actual V2G power being supplied through these profiles. Thus, after accounting for above two deductions, the V2G profiles shown contains energy corresponding to 24.3, 30, and 26.2% of the average battery capacities, respectively, at the three penetration ratios of 25, 50, and 100%. The relative G2V and V2G MW values of the aggregation under the various scenarios are summarized in Table 11.10. It can be observed that the V2G profiles at the three penetration ratios are not proportionately modified. For example, neither the V2G peak is proportionately altered with the penetration ratios nor the shifting of V2G peak times with the increase in V2G power from 1.44 to 6.6 kW is proportionate with the variation in penetration ratios. This is due to the presence of heterogeneity in the mobility attributes, resulting in the changed G2V/V2G energy equilibrium of the aggregation at these penetration levels. The important characteristics of these profiles due to changed equilibrium at these penetrations are shown in Table 11.11.

11.3.3.2 G2V Profiles

Figure 11.5 shows the G2V profiles of the aggregation at the two terminal charge power levels of 2.5 and 6.6 kW of the considered range under the three penetration ratios. This G2V power is the sum of energy required by the EVs for driving as well as power consumed from the batteries in V2G supply. It can be observed from the profiles that, as a result of increased charging rate, the G2V peak increases as well

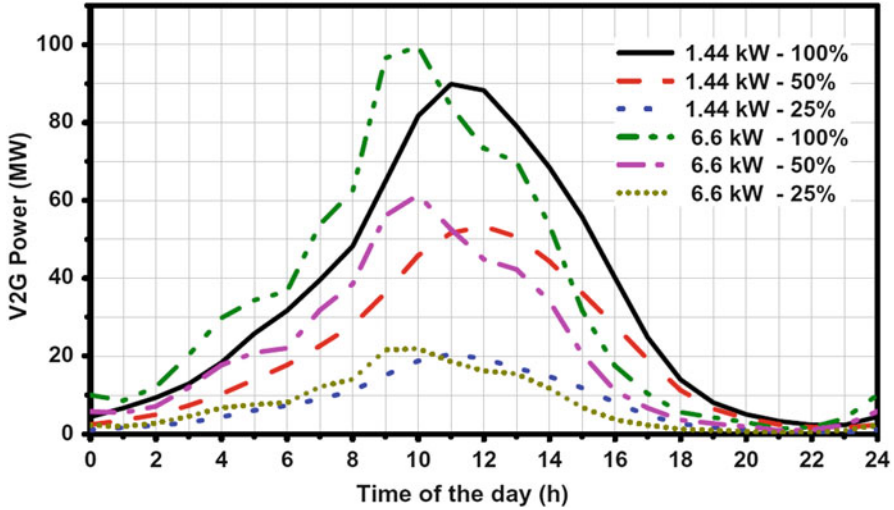


Fig. 11.4 V2G profiles of aggregation

Table 11.10 V2G and G2V energy balance of the aggregation

Particular	MWs			% of total battery capacity		
	25%	50%	100%	25%	50%	100%
V2G power by aggregation	182.53	503.08	824.70	24.27	29.93	26.17
Aggregated inverter loss	13.74	37.87	62.07	1.83	2.25	1.97
Driving consumption of aggregation	403.57	835.45	1645.89	53.66	49.71	52.24
Total G2V demand of aggregation	599.85	1376.40	2532.67	79.75	81.90	80.38

Table 11.11 Characteristics of V2G profiles

V2G power level (kW)	V2G peak power (MW)			Peak time			V2G duration (h)			Total V2G power (MW)		
	25%	50%	100%	25%	50%	100%	25%	50%	100%	25%	50%	100%
1.44	20.48	53.32	89.88	11:00	12:00	11:00	2.98	4.11	3.37	182.535	503.084	824.699
1.64	20.96	54.23	94.55	11:00	12:00	11:00	2.62	3.61	2.96			
1.92	21.82	56.23	94.80	10:00	11:00	11:00	2.24	3.08	2.53			
2.5	21.93	57.60	95.59	10:00	11:00	10:00	1.72	2.37	1.94			
3.3	22.60	59.63	98.99	10:00	10:00	10:00	1.30	1.79	1.47			
6.6	23.24	61.39	99.55	10:00	10:00	10:00	0.65	0.90	0.73			

as shifts toward left with the increase in charging power level from 2.5 to 6.6 kW at all the penetration ratios. Conversely, the minimum G2V load decreases and shifts toward early hours with the increase of charging power. The characteristic thing to be noted that the average increase in G2V peak or decrease in minimum G2V load is not proportionate at the three penetration ratios at various charge power levels.

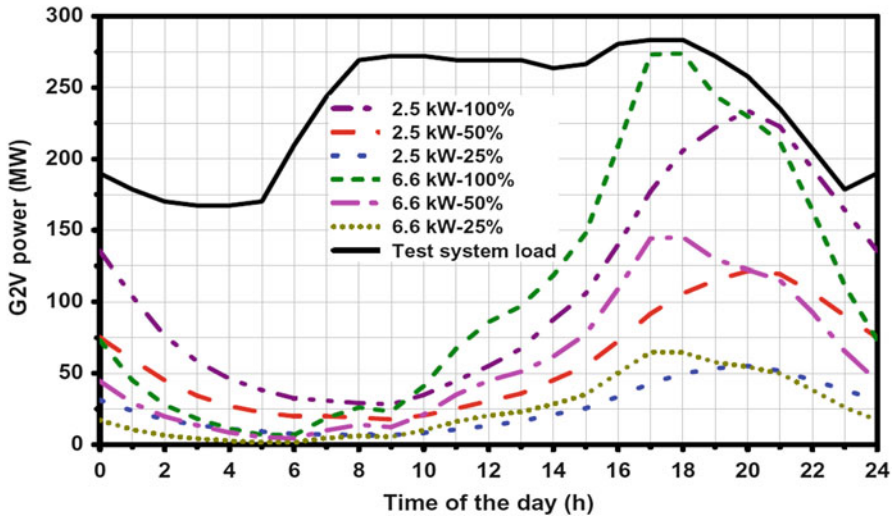


Fig. 11.5 G2V profiles of aggregation

Table 11.12 Characteristics of G2V profiles

G2V power level (kW)	Peak G2V power (MW)			Peak time			Least G2V power (MW)			Time of occurrence		
	25%	50%	100%	25%	50%	100%	25%	50%	100%	25%	50%	100%
2.5	55.15	121.61	233.74	20:00	20:00	20:00	6.64	17.67	28.23	09:00	09:00	09:00
3.3	57.97	129.76	245.03	19:00	19:00	19:00	4.62	14.15	20.36	06:00	09:00	06:00
6.6	64.90	145.08	273.91	17:00	18:00	18:00	1.58	4.30	06.82	05:00	06:00	06:00

Again, this is on account of heterogeneity in the vehicles’ attributes at the three penetration ratios, varying the energy equilibrium. The variation in the concentration of different capacity (types) EVs alters the G2V/V2G capacities of the aggregation under the various penetration scenarios. Table 11.12 summarizes the characteristics of resulting G2V profiles of the EV aggregation.

11.3.3.3 Effect of V2G and G2V Profiles Integration on Grid Load and Electricity Pricing

Integration of the resulting V2G and G2V profiles with the system will modify the daily load pattern. The variations in market clearing volume (MW) due to this can alter the electricity market clearing price (MCP) due to the tweaks in unit commitment. A single-sided auction mechanism has been employed to determine the hourly market clearing price (MCP) Gutierrez et al (2005). Modified IEEE 30-Bus system Shahidehpour et al (2002) composed of nine generating units is taken as the test system to demonstrate the effect on electricity market price. The combined

Table 11.13 Generator data

Generating unit	P_{\min} (MW)	P_{\max} (MW)	Marginal cost (\$/MWh)
G1	7	28	6.010
G2	14	56	8.005
G3	20	84	10.004
G4	25	100	13.345
G5	20	130	16.504
G6	15.2	76	18.012
G7	10	55	25.928
G8	4	20	37.575
G9	2.4	12	39.922

Table 11.14 Characteristics of net load on the system

Charge/ discharge power (kW)	Highest slump in load (MW)			Time of highest slump			Maximum hike in load (MW)			Time of maximum hike		
	25%	50%	100%	25%	50%	100%	25%	50%	100%	25%	50%	100%
2.5	13.56	34.88	60.78	10:00	10:00	10:00	54.36	119.16	230.00	20:00	20:00	20:00
3.3	14.13	40.74	65.42	10:00	10:00	10:00	56.95	126.72	240.31	19:00	19:00	19:00
6.6	16.03	43.82	73.24	09:00	09:00	09:00	63.41	141.50	268.32	18:00	18:00	18:00

generating capacity of the system is 561 MW. Generator limits, as well as their marginal cost of generating electricity, are presented in Table 11.13. The generator data are obtained from Djurovic et al (2012); Qiaozhu Zhai et al (2009). Hourly conventional load, expected to be fixed, on the system is computed for a regular winter weekday according to IEEE reliability test system Wong et al (1999) taking daily peak loads value from Shahidehpour et al (2002). Generators are assumed to bid their true marginal cost of generating power. The conventional daily load curve thus obtained for the selected modified IEEE 30-Bus test has been shown in Fig. 11.5 via solid black line.

The effect of integration of resulting V2G and G2V profiles with the selected test system on hourly loading and electricity market price is quantified in Tables 11.14 and 11.15, respectively. The two distinct attributes of the resulting system load and hourly MCP are: (1) reduction in net load and hence the MCP in the morning hours due to V2G supply of the aggregation with arrival of vehicles at workplace, and (2) rise in net load and hence the MCP due to G2V demand of the aggregation with arrival of vehicles at home. Table 11.14 summarizes the relative MW values of maximum hike and reduction in the original test load as well as their timings due to the integration of V2G and G2V profiles, under the three penetration scenarios.

Table 11.15 Characteristics of electricity market pricing

G2V and V2G power level (kW)	MCP reduction intervals			New MCP (\$/MWh)	Old MCP (\$/MWh)	MCP hike intervals			New MCP (\$/MWh)	Old MCP (\$/MWh)
	25%	50%	100%			25%	50%	100%		
2.5						03:00-05:00	03:00-05:00	03:00-05:00	13.345	10.004
						14:00-16:00	14:00-16:00	24:00-02:00	16.504	13.345
						20:00-22:00	20:00-23:00	14:00-16:00	16.504	13.345
	08:00-13:00	08:00-14:00	08:00-14:00	13.345	16.504			23:00-24:00	16.504	13.345
								21:00-23:00	18.012	13.345
3.3								20:00-21:00	25.928	13.345
								17:00-18:00	18.012	16.504
								18:00-20:00	25.928	16.504
						03:00-05:00	03:00-05:00	03:00-05:00	13.345	10.004
	08:00-13:00	08:00-14:00	05:00-06:00	10.004	13.345	14:00-16:00	14:00-16:00	24:00-01:00	16.504	13.345
6.6						20:00-22:00	20:00-23:00	14:00-16:00	16.504	13.345
								22:00-24:00	16.504	13.345
	08:00-13:00	08:00-14:00	08:00-13:00	13.345	16.504			21:00-22:00	18.012	13.345
								20:00-21:00	25.928	13.345
								16:00-17:00	18.012	16.504
							18:00-20:00	25.928	16.504	
							03:00-04:00	13.345	10.004	
								14:00-16:00	16.504	13.345
								22:00-24:00	16.504	13.345
05:00-06:00	05:00-06:00	05:00-06:00	10.004	13.345				22:00-23:00	18.012	13.345
								20:00-21:00	25.928	13.345
08:00-12:00	08:00-12:00	08:00-12:00	13.345	16.504				16:00-17:00	18.012	16.504
								19:00-20:00	25.928	16.504
								17:00-18:00	37.575	16.504
								18:00-19:00	39.922	16.504

The lower charge and discharge power level results in a flatter G2V and V2G profiles, respectively, resulting in a lesser increase of electricity market price with G2V as scheduling of costly generators are avoided. The two critical mobility attributes namely the driven distance and the base case arrival time at homes are independent of each other. Thus, the equilibrium of various EVs regulates the amount of V2G support and hence the net load on the system and hourly market prices with the integration of G2V and V2G profiles at various charge/discharge power levels. The above analysis concludes that the V2G support is not only dependent on the number of vehicles available to support the grid but is also dependent on the heterogeneity of the aggregation where battery electric vehicles (BEVs) may contribute more to V2G than plug-in hybrid electric vehicles (PHEVs), an important factor necessary to be incorporated to create any future robust model of EV dominated transportation system in order to accurately predict the fleet level effects on the grid.

11.4 Electric Vehicles Charging and Discharging Coordination for Reserve Capacity Commitment

This section presents the coordination of the EV aggregation during the charging and discharging phases to obtain the MW capacity that can be contracted as the capacity commitment (energy and reserve) in the volatile ancillary services market. After accounting for the driving consumption in transportation, the available battery capacity is the storage that can be supplied to the grid through V2G as a coordinated aggregation to produce MW level effect on the grid. Based on the mobility pattern defined in the previous section, the two parking places of home and work can be considered as the two operational places to simulate the G2V and V2G activities. The changeable locations of vehicles also suggest that the grid services function can be segregated based on the zone of operation (control area) of vehicles. In view of this, the aggregation of vehicles can either charge (G2V) at home and discharge (V2G) at work, or it can charge (G2V) at work while discharge (V2G) at home.

As discussed in the previous section, the vehicles arrive at the two places—home and work as per the pattern shown in Figs. 11.1 and 11.3 respectively, all over the day. Let there is n work as well as home arrival times and the number of vehicles arriving at either of the two places during these times are:

$$N_1, N_2, N_3, \dots, N_n$$

The Charging (G2V) Phase Let the selected charging and discharging power levels (kW) for the aggregation of vehicles are P_c and P_d . Then, the CP phase charging power of the aggregation in MW arriving at a particular time n is given by,

$$MW_{CP}^c = \left(\frac{P_c}{1000} \right) \cdot N_n \quad (11.3)$$

and the CT phase charging power of the aggregation in MW arriving at a particular time n

$$MW_{CT}^c = \left(\frac{P_c}{1000} \right) \cdot \left(\frac{MWh_{CT}^c}{B} \right) \quad (11.4)$$

where B is the average battery capacity of the vehicles considered in the aggregation.

Total charging duration of the aggregation is given by,

$$T^c = \left(\frac{MWh_{CP}^c}{MW_{CP}^c} \right) + \left(\frac{MWh_{CT}^c}{MW_{CT}^c} \right) = T_{CP}^c + T_{CT}^c \quad (11.5)$$

where MWh_{CP}^c and MWh_{CT}^c are the total energy required by the aggregation arriving at particular time in CP and CT phase of charging, respectively.

The Discharging (V2G) Phase The discharging power of the aggregation in MW arriving at a particular time n is,

$$MW_{dis} = \frac{P_d}{1000} \cdot N_n \quad (11.6)$$

and, the total discharging duration of the aggregation,

$$T^d = \frac{MWh_n^{dis}}{MW_{dis}} \quad (11.7)$$

where MWh_n^{dis} is the total V2G energy made available by the aggregation arriving at time n .

Determination of Capacity Reserve Let, there are n variables (α) along the n arrival times for each of the two CP and CT phases of charging, i.e., $\alpha_{CP}(n)$ and $\alpha_{CT}(n)$, respectively. There are total 1440 min (denoted by t) in a day's timeline starting from 00:00 till 23.59. For a given total charging duration of the aggregation arriving at various times of the day, the α variables take the value unity or zero as per the following conditions:

$$\alpha_{CP} = \begin{cases} 1 & \forall n \leq t \leq (n + T_{CP}^c) \\ 0 & \text{otherwise} \end{cases} \quad (11.8)$$

$$\forall t = 1, 2, 3, \dots, 1440$$

$$\alpha_{CT} = \begin{cases} 1 & \forall (n + T_{CP}^c) \leq t \leq (n + T^c) \\ 0 & \text{otherwise} \end{cases} \quad (11.9)$$

$$\forall t = 1, 2, 3, \dots, 1440$$

Here, n is the n^{th} arrival time of the vehicles. The total charging (G2V) power drawn by the EVs at any minute of the day is obtained as,

$$MW^c = \sum_{i=1}^n [(\alpha_{CP}(i) \cdot MW_{CP}^c) + (\alpha_{CT}(i) \cdot MW_{CT}^c)] \quad (11.10)$$

and the total discharged power (V2G) of the EVs at any minute of the day,

$$MW^d = \sum_{i=1}^n [\alpha_{CP}(i) \cdot MW_{dis}] \quad (11.11)$$

Hence, the net power supplied or drawn from the grid at any minute of the day is given by,

$$MW^{\text{Net}} = MW^c - MW^d \quad (11.12)$$

Nonetheless, if only unidirectional flow of power during charging (G2V) is possible due to infrastructure limitations, the $MW^d = 0$ and,

$$MW^{\text{Net}} = MW^c \quad (11.13)$$

The capacity reserve (generation/demand) for any m minutes time-interval in a day's timeline can be obtained by taking the average value of net power supplied/drawn from the grid over that m minutes, i.e.,

$$\text{Capacity reserve (generation/demand)} = \overline{MW}^{\text{Net}} \quad \forall t \in (1, 2, 3, \dots, m) \quad (11.14)$$

The reserve capacity of the aggregation at any moment is dependent upon vehicles' arrival patterns at home and work as shown in Figs. 11.1 and 11.3, respectively. Consequently, when the aggregation chooses to charge at work and discharge at home, the demand capacity (G2V) of the reserve will be dominating the generation capacity (V2G) of reserve at the morning hours while vice versa in the evening. Conversely, when the aggregation is selected

(continued)

to charge at home and discharge at work, the demand capacity (G2V) of the reserve will be dominating the generation capacity (V2G) of reserve at the evening hours while vice versa in the morning. The ancillary services market for the capacity reserve is a volatile high-value market. Thus, for a defined mobility pattern a capacity commitment (energy and reserve) in these competitive services market on a long-term basis could yield a notable revenue stream, in addition to increasing the grid reliability.

11.5 Load Leveling Through Charging and Discharging Coordination

The load levelization simplifies the load forecasting and dispatch exercises in the system operation by reducing the complexities associated with the oscillating load, and thereby the regulation services requirements. With a defined mobility pattern of home–work commute with work and home as the two parking slots available for G2V and V2G activities, the charging and discharging modes of EV aggregation can be coordinated to fill the valley(s) and shave the peak(s) of a fluctuating load with a purpose of its levelization. This can be realized by enacting the G2V (charging) mode and V2G (discharging) mode of the aggregation respectively, during the valley periods and peaking times of the original load.

Let us construe a case of coordinating the charging of the vehicles during their availability at home (G2V) and discharging during their availability at the workplace (V2G), with a purpose of valley filling and peak shaving, respectively. The assumptions on vehicles and its parameters are shown in Table 11.16.

The pattern of arrival of vehicles at home and the workplace is previously shown in Figs. 11.1 and 11.3, respectively. In this case, a total 24 arrival times are considered for both home and workplace arrival of vehicles. With the total number

Table 11.16 Assumptions on vehicle parameters

Parameter	Value
Type of vehicle	Nissan LEAF electric car (BEV)
Total number of vehicles	0.25 million
Battery capacity	24 kWh
Battery capacity with 80% DoD	19.2 kWh
Capacity required for 20 km range buffer	3.632 kW
Net available capacity for driving	15.568 kWh
Average home–work commute distance	27.5 km
Energy consumed in home–work commute	5 kWh
Net available battery capacity for V2G	10.567 kWh

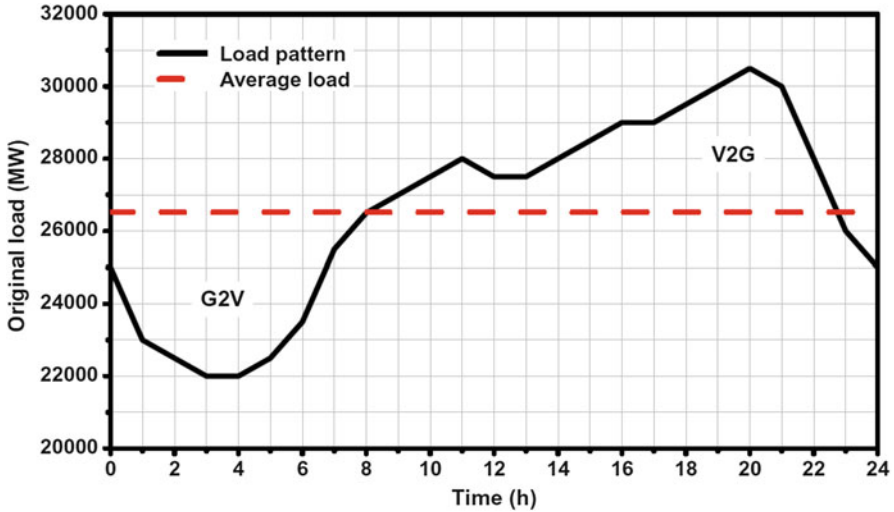


Fig. 11.6 Hourly load pattern of CAISO load (Monday, June 12, 2017)

of vehicles assumed to be 0.25 million in the system, the actual number of vehicles arriving at these 24 arrival times can be obtained from the above patterns. Here, the home parking, workplace parking, and travel duration constraints are assumed to be 15, 7, and 2 h, respectively. Figure 11.6 shows the demand curve of a typical day (Monday, June 12, 2017) of California Independent System Operator (CAISO) system CAISO (2017), with the dashed line showing the average load of 26,520 MW of the day. The maximum demand is 30,500 MW occurring at hour 20:00 while the minimum demand being 22,000 MW occurring at hours 03:00 and 04:00. Between the two demands, the load pulsates requiring ramping up and down of the generation sources in order to follow the load pattern.

In order to levelize the load around the average value, the load points (MWs) above the average load has to be curtailed through V2G (peak shaving), while the load points (MWs) below the average values are to be lifted through G2V (valley filling) by the aggregation. Thus, from Fig. 11.6, the V2G supply is required between hours 08:00 and 23:00, while the G2V is required between the hours 00:00–08:00 and 23:00–24:00, in order to levelize the load around the average. For simplification of G2V and V2G coordination, the charging and discharging power per vehicle are set to 10.60 and 15.57 kW, respectively, so that the aggregation is able to discharge and charge completely to the limits considered within an hour. These charging powers fall in the gamut of AC Level 2 gamut of EV charging standards (Table 11.5). The vehicles are charged and discharged with constant power charging approach.

Let the various hours of the day is denoted by h_n , where $n \in (1, 2, 3, \dots, 24)$, then MW drawn, i.e., G2V by the aggregation in an hour h_n to h_{n+1} ,

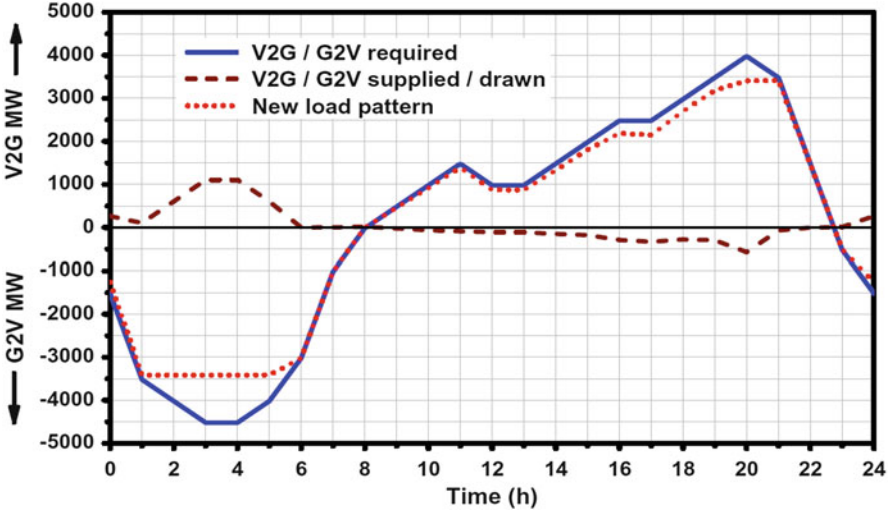


Fig. 11.7 V2G and G2V MWs required as well as supplied by the aggregation at various times

$$MW_{G2V} = \left(\frac{10.60}{1000} \right) N_{h_n} \tag{11.15}$$

and the MW supplied, i.e., V2G by the aggregation in an hour h_n to h_{n+1} ,

$$MW_{V2G} = \left(\frac{15.57}{1000} \right) N_{h_n} \tag{11.16}$$

Here, N_{h_n} is the number of vehicles arriving (hence available) at hour n of the day.

The vehicles are scheduled V2G and G2V modes with the set charging and discharging power levels, as per the constraints work and home parking duration specified. It should be noted that as the vehicles are primarily accompanied by transportation (driving) energy consumption, the V2G support MWs by the aggregation would inherently be lesser than the charging demand (G2V support). In other words, the total G2V demand from the grid is the sum of driving energy consumption and the energy supplied through V2G. The accessibility of net V2G and G2V MWs for peak shaving and valley filling respectively is limited by the total number of vehicles in the system as well as the pattern of arrival of vehicles which governs the availability of number vehicles at the two locations for charging and discharging. Therefore, here, the net V2G/G2V supplied/drawn by the scheduling the vehicles for peak shaving and valley filling respectively during the various hours is lesser than the V2G/G2V required to completely levelize the load around the average, as shown in Fig. 11.7. In this figure, for depiction, the average load is shown by zero and pattern of G2V and V2G required are plotted below and above the zero average, respectively. Nonetheless, a significant amount of peak shaving and valley filling is achieved thereby leveling the load. Table 11.17 summarizes the relative

Table 11.17 MW proportions in V2G/G2V coordination

Particular	Value
V2G MWs supplied by the EV aggregation	2572.37
Travel demand of the EV aggregation (MW)	1248.87
G2V MWs drawn by the EV aggregation	3821.16

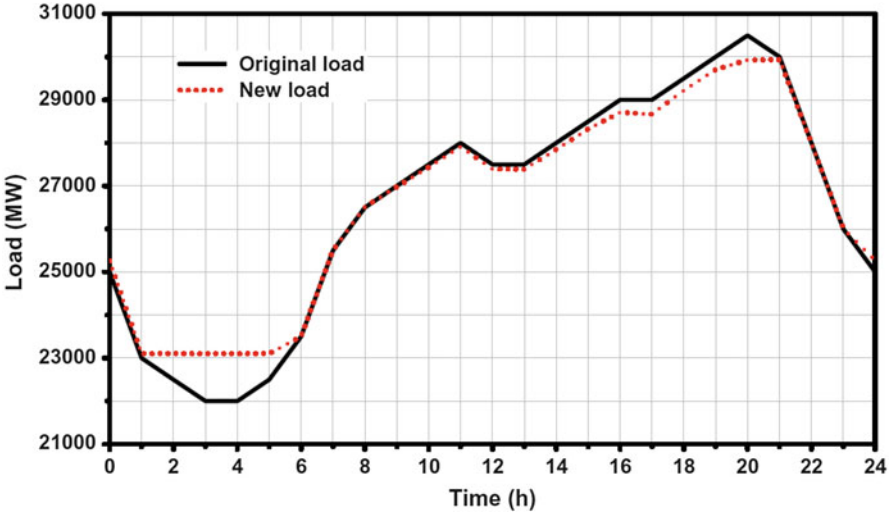


Fig. 11.8 New equalized load pattern

MW proportions of G2V and V2G energy transfer in this scheme for load leveling. Figure 11.8 shows the new hourly load curve of the day after the levelization through V2G and G2V coordination.

Conventionally, the ramp up and ramp down energy and reserve requirements to match the fluctuating load throughout the day are provided by expensive and slow response coal, gas, or fossil fuel based power sources. The oscillating and unpredictable nature of load necessitates procurement of these costly ancillary services (energy and reserve capacity) by the system operator to maintain the stable and reliable operation of the interconnected system. The increased cost of electricity is ultimately ended up being passed on to the final consumers. The load leveling mechanism through V2G and G2V coordination by a large pool of EVs as demonstrated can be an effective measure to reduce the dependability of ramping commitments on traditional sources, thereby reducing the ultimate cost of electricity to the consumers. In addition, the G2V and V2G energy storage and transactions take place on the distribution side (receiving end) avoiding the transmission line congestion, mostly at the peaking times.

11.6 Electric Vehicle Grid Interfacing to Enable Support Through Power Storage

Figure 11.9 shows the representative schematic of the electric vehicle and electric utility interfacing to facilitate the grid support services through aggregated EV storage. The EVs offer the advantage of high ramp up and ramp down speed capabilities but at the same time possess the limitations of changeable availability affecting the contract sizes and absence of stabilizing inertia as of the large generators. This makes them appropriate for short-term high-value ancillary services markets Kempton and Tomić (2005a) like regulation and spinning reserves instead for the base load sources, as shown in Fig. 11.9.

The charging points having the ability to enable two-way communication between the charging station and the EV to limit the charging current to the safe limits are also termed as the electric vehicle supply equipment (EVSE). In order to have control over the charge as well as discharge rates of the vehicle battery, the EVSE must be designed to have the bidirectional power and communication flow capabilities. Also, to support V2G, the EVSE should be designed to have the capability to handle different charge/discharge power levels and support AC as well as DC power transfer to/from the vehicle as per the infrastructure requirements.

The standard battery capacity of an electric vehicle is only in the range of few kilowatt hours, creating negligible impact at the grid level operations. The V2G support services would require a controllable capacity of MWs to have a substantial impact on the system. This is possible only with the aggregated battery storage necessitating the grouping of a large number of available EVs at the moment. Also, it is almost impractical for the system operator to interact with each individual vehicle. Thus, an interfacing entity called vehicle aggregator Guille and Gross (2009); Lopes et al (2011) is proposed, for managing the groups of battery storage to provide overall load (G2V) and generation (V2G) services to the electric utility (system operator). To the system operator, the aggregator provides a single point of contact—managing a resource of rapidly controllable electric reserve and its

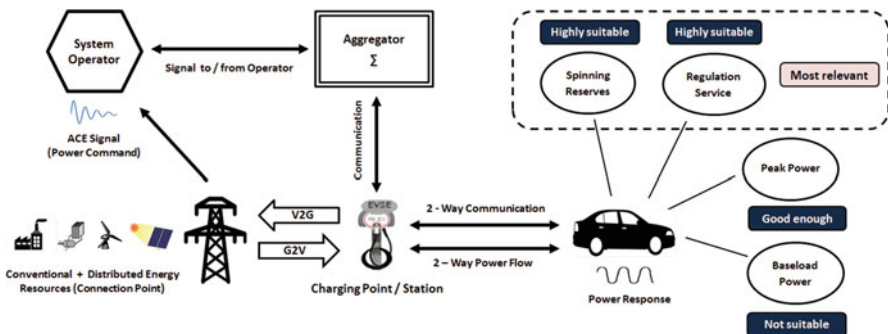


Fig. 11.9 Schematic of EV and electric utility interactions for grid support through V2G

participation in grid support services. Principally, the vehicle aggregator would be in control of (1) location monitoring of vehicles, (2) tracking their grid connectivity, (3) integrating participants to ensure sufficient capacity, (4) ensuring their participation, (5) communication/control (command) signals from/to the system operator, (6) establishing contracts with the operator, and (7) coordinating the payment streams down to the connected vehicles for the grid services. The system requirement for this include added communication and controls with the electric utility to ensure the energy transfer between the vehicle owner and system operator in an optimal way. An unregulated utility transacting electricity or an independent third party entity like an automobile manufacturer, a battery manufacturer, or a mobile network provider having expertise in communication functions and automated customer transactions may serve as a vehicle aggregator in the future scenario Briones et al (2012); Kempton and Tomić (2005b).

Justification of the economic feasibility of V2G is contingent upon numerous factors. High battery cost, long charging time, range anxiety, costly charging infrastructure, etc. are the first few hurdles in the greater EV adoption. However, in V2G, the electric utilities or in turn the vehicle aggregators will have control and access to charging/discharging of vehicle batteries for the purpose of improving the system reliability through grid support. Thus, the bidirectional power flow in V2G allows the commitment of energy and capacity services via the grid-connected vehicles for which the aggregator and hence the vehicle owners will be compensated. The value created on the part of these services would be a vital motivation toward consumers' willingness to participate in V2G. Not to mention, the V2G support services should be in addition to the primary function of the vehicles, i.e., transportation, in order to not to jeopardize the customers' comfort of vehicle utilization in travel.

Nomenclature

Abbreviations, Acronyms, & Symbols

α_{CP}	Variable along CP phase of charging
α_{CT}	Variable along CT phase of charging
\overline{MW}^{Net}	Capacity reserve (generation/demand)
AER_{avg}^D	Average value of AER achievable by vehicle aggregation in downtown driving
AER_{avg}^E	Average value of AER achievable by vehicle aggregation in expressway driving
AER_{avg}^R	Average value of AER achievable by vehicle aggregation in road driving
AER_{avg}^{Tr}	Average value of AER achievable by vehicle aggregation in traffic driving

B	Average battery capacity of the vehicles considered in the aggregation
d_m^t	Driven distance by the m^{th} distance group of vehicles arriving at time t
E^τ	Energy consumed in driving by the EV aggregation arriving at time τ
E^t	Charging demand of EV aggregation arriving at time t
E_{avg}	Average energy consumed by the vehicle
E_{avg}^D	Average value of energy consumed per km by the vehicle aggregation in downtown driving
E_{avg}^E	Average value of energy consumed per km by the vehicle aggregation in expressway driving
E_{avg}^R	Average value of energy consumed per km by the vehicle aggregation in road driving
$E_{\text{avg}}^{\text{Tr}}$	Average value of energy consumed per km by the vehicle aggregation in traffic driving
h_n	n^{th} hour of the day
$k_m^{D\tau}$	km traveled by m^{th} mileage group of vehicle aggregation arriving at time τ in downtown driving
$k_m^{E\tau}$	km traveled by m^{th} mileage group of vehicle aggregation arriving at time τ in expressway driving
$k_m^{R\tau}$	km traveled by m^{th} mileage group of vehicle aggregation arriving at time τ in road driving
$k_m^{\text{Tr}\tau}$	km traveled by m^{th} mileage group of vehicle aggregation arriving at time τ in traffic driving
MW^c	Total charging (G2V) power drawn by the EVs at any minute of the day
MW^d	Total discharged power (V2G) of the EVs at any minute of the day
MW^{Net}	Net power supplied or drawn from the grid at any minute of the day
MW_{CP}^c	CP phase charging power of the aggregation in MW
MW_{CT}^c	CT phase charging power of the aggregation in MW
MW_{dis}	Discharging power of the aggregation in MW
MW_{G2V}	MW drawn by the aggregation
MW_{V2G}	MW supplied by the aggregation
MWh_{CP}^c	Energy required by the aggregation in CP phase of charging
MWh_{CT}^c	Energy required by the aggregation in CT phase of charging
$\text{MWh}_n^{\text{dis}}$	V2G energy made available by the aggregation arriving at time n
n	n^{th} arrival time of the vehicles
N_{h_n}	number of vehicles arriving at hour n of the day
n_m^t	Number of m^{th} distance group of vehicles arriving at time t
N_n	Number of vehicles arriving at a particular time n
P_c	Selected charging power level (kW) for the aggregation of vehicles
P_d	Selected discharging power level (kW) for the aggregation of vehicles
pc_m^τ	Percentage of m^{th} mileage group of vehicle aggregation arriving at time τ
T^c	Total charging duration of the aggregation
T^d	Total discharging duration of the aggregation
T_{CP}^c	CP phase charging duration of the aggregation

T_{CT}^c	CT phase charging duration of the aggregation
AER	All-electric range
BEV	Battery electric vehicle
CAISO	California Independent System Operator
CC	Constant current
CP	Constant power
CT	Constant time
CV	Constant voltage
DCFC	Direct current fast charging
DoD	Depth of discharge
EIA	Energy Information Administration
EPRI	Electric Power Research Institute
EV	Electric vehicle
EVSE	Electric vehicle supply equipment
G2V	Grid-to-vehicle
GHG	Greenhouse gas
ICE	Internal combustion engine
IEA	International Energy Agency
MCP	Market clearing price
MPG	Miles per gallon
PHEV	Plug-in hybrid electric vehicle
SAE	Society of Automotive Engineers
SOC	State-of-charge
T&D	Transmission and distribution
V2G	Vehicle-to-grid

Acknowledgements The authors thank Rishil Lakhe, third year B.Tech. Electrical Engineering student from Sardar Vallabhbhai National Institute of Technology Surat, Surat, India, for technical assistance in preparing Sects. 11.1 and 11.5 of the chapter.

References

1. Briones A, Francfort J, Heitmann P, Schey M, Schey S, Smart J (2012) Vehicle-to-grid (V2G) power flow regulations and building codes review by the Avta. Technical report INL/EXT-12-26853, Idaho National Laboratory, U.S. Department of Energy National Laboratory, Idaho Falls, Idaho [Online]. Available <https://energy.gov/eere/vehicles/downloads/avta-vehicle-grid-power-flow-regulations-and-building-codes-review>
2. CAISO (2017) California Independent System Operator [Online]. <http://www.caiso.com/Pages/default.aspx>
3. Darabi Z, Ferdowsi M (2011) Aggregated impact of plug-in hybrid electric vehicles on electricity demand profile. *IEEE Trans. Sustainable Energy* 2(4):501–508
4. Djurovic MZ, Milacic A, Krsulja M (2012) A simplified model of quadratic cost function for thermal generators. In: *Annals and proceedings of DAAAM international*, Vienna, vol 23, No 1
5. Duvall M et al (2011) Transportation electrification: a technology overview. Technical report, CA: 2011.1021334, Electrical Power Research Institute, Palo Alto, CA, pp 3.1–3.2, 5.10

6. Edenhofer O, Pichs-Madruga R, Sokona Y et al (2012) Renewable energy sources and climate change mitigation. Summary for policymakers and technical summary, Potsdam Institute for Climate Impact Research, The Intergovernmental Panel on Climate Change
7. Eggleston S, Buendia L, Miwa K et al (2006) 2006 IPCC guidelines for national greenhouse gas inventories, prepared by the national greenhouse gas inventories programme. IPCC report, The Intergovernmental Panel on Climate Change, IGES, Japan
8. EIA (2013) Annual Energy Outlook 2013 - with projections to 2040. Report DOE/EIA-0383(2013), U.S. Energy Information Administration, Washington, DC
9. EIA (2017) How much electricity is lost in transmission and distribution in the United States? U.S. Energy Information Administration. <https://www.eia.gov/tools/faqs/faq.php?id=105&t=3> [Online]. Accessed May 2017
10. EIA (2017) What is U.S. electricity generation by energy source? U.S. Energy Information Administration. <https://www.eia.gov/tools/faqs/faq.php?id=427&t=3> [Online]. Accessed May 2017
11. Federal Register (2010) Light-duty vehicle greenhouse gas emission standards and corporate average fuel economy standards; Final Rule, p 25330. Federal Register/Vol 75, No. 88, Part - II: Environmental Protection Agency, Department of Transportation
12. Guille C, Gross G (2009) A conceptual framework for the vehicle-to-grid (V2G) implementation. Energy Policy 37(11):4379–4390
13. Gutierrez G, Quinonez J, Sheble GB (2005) Market clearing price discovery in a single and double-side auction market mechanisms: Linear programming solution. In: Proceedings of 2005 IEEE Russia power technologies, St. Petersburg
14. IEA (2011) Technology roadmap: electric and plug-in hybrid electric vehicles. Technical report, International Energy Agency, France
15. Jain P, Jain T (2014) Assessment of electric vehicle charging load and its impact on electricity market price. In: 2014 international conference on connected vehicles and expo (ICCVE), Vienna, pp 74–79
16. Jain P, Jain T (2014) Impacts of G2V and V2G power on electricity demand profile. In: 2014 IEEE international electric vehicle conference (IEVC), Florence, pp 1–8
17. Jain P, Jain T (2016) Development of V2G and G2V power profiles and their implications on grid under varying equilibrium of aggregated electric vehicles. Int J Emerg Electr Power Syst 17(2):101–115
18. Kalhammer FR, Kamath H, Duvall M, Alexander M, Jungers B (2009) Plug-in hybrid electric vehicles: promise, issues and prospects. In: Proceedings of EVS24 international battery, hybrid and fuel cell electric vehicle symposium, Stavanger, pp 1–11
19. Kempton W, Tomic J (2005) Vehicle-to-grid power fundamentals: calculating capacity and net revenue. J Power Sources 144(1):268–279
20. Kempton W, Tomic J (2005) Vehicle-to-grid power implementation: from stabilizing the grid to supporting large-scale renewable energy. J Power Sources 144(1):280–294
21. Lopes JAP, Soares FJ, Almeida PMR (2011) Integration of electric vehicles in the electric power system. Proc IEEE 99(1):168–183
22. Markowitz M (2013) Wells to wheels: electric car efficiency. <https://matter2energy.wordpress.com/2013/02/22/wells-to-wheels-electric-car-efficiency/> [Online]. Accessed May 2017
23. Naughton N (2015) Average U.S. mpg edges up to 25.5 in May. Automotive News. <http://www.autonews.com/article/20150604/OEM05/150609925/average-u.s.-mpg-edges-up-to-25.5-in-may> [Online]. Accessed May 2017
24. NHTS (2001) National Household Travel Survey (NHTS), U.S. Department of Transportation [Online]. Available <http://nhts.ornl.gov>
25. Pasaoglu GK, Fiorello D, Martino A, Scarcella G, Alemanno A, Zubaryeva A, Theil C (2012) Driving and parking patterns of European car drivers - a mobility survey. Technical report JRC77079, EUR - scientific and technical research reports, Institute for Energy and Transport, European Commission, Joint Research Centre (2012) [Online]. Available <http://publications.jrc.ec.europa.eu/repository/handle/JRC77079>

26. Qiaozhu Zhai Q, Guan X, Yang J (2009) Fast unit commitment based on optimal linear approximation to nonlinear fuel cost: error analysis and applications. *Electr Power Syst Res* 79(11):1604–1613
27. RWTH (2010) WP:1.3 Parameter manual. V05 ed., Grid for vehicles (G4V), RWTH Aachen [Online]. Available <http://www.g4v.eu/>
28. Sachen R (2015) EV vs gas - part 2 emissions. Sunspeed Enterprises. <http://sunspeedenterprises.com/ev-vs-gas-part-2-emissions/> [Online]. Accessed May 2017
29. Shahidehpour M, Yamin H, Li Z (2002) Example systems data. In: *Market operations in electric power systems: forecasting, scheduling, and risk management*. Wiley, New York. IEEE, appx. D, sec. D.4, pp 477
30. Simpson C (2011) Battery charging. Literature No. SNVA557, 2011, National Semiconductor, Texas Instrument [Online]. Available <http://www.ti.com/lit/an/snva557/snva557.pdf>
31. Tesla (2017) <https://www.tesla.com/models> [Online]. Accessed May 2017
32. TIAX LLC (2007) Full fuel cycle assessment, well to tank energy inputs, emissions, and water impacts. Consultant report (draft), California Energy Commission, Cupertino, CA
33. Wong P, Albrecht P, Allan R, Billinton R, Chen Q, Fong C, Haddad S, Li W, Mukerji R, Patton D, Schneider A, Shahidehpour M, Singh C (1999) The IEEE reliability test system-1996. *IEEE Trans Power Syst* 14(3):1010–1020
34. Young K, Wang C, Wang LI, Strunz K (2013) Electric vehicle battery technologies. In: *Electric vehicle integration into modern power networks*. Power electronics and power systems, 1st edn. Springer, New York